Prediction of Non-Catalytic Esterification of Free Fatty Acids Comprising Karanja Oil Using Ann

Daniel Chuquin-Vasco [1,] *, Ana Sancho[2], Nelson Chuquin-Vasco[3], Juan Chuquin-Vasco[3] and Cristina Calderón-Tapia [4]

[1] Escuela Superior Politécnica de Chimborazo (ESPOCH), Facultad de Ciencias ,Grupo de investigación en seguridad, ambiente e ingeniería (GISAI); daniel.chuquin@espoch.edu.ec (D.CH.V);
[2] EP-Empresa Municipal de Agua Potable y Alcantarillado de Ambato (EP-EMAPA)
[3] Escuela Superior Politécnica de Chimborazo (ESPOCH),Facultad de Mecánica, Grupo de investigación en seguridad, ambiente e ingeniería (GISAI);nelson.chuquin@espoch.edu.ec (N.CH.V); juan.chuquin@espoch.edu.ec(J.CH.V)
[4] Escuela Superior Politécnica de Chimborazo (ESPOCH), Facultad de Ciencias, Grupo de investigación Desarrollo para el ambiente y Cambio Climático (GIDAC); cristina.calderont@espoch.edu.ec (C.C.T);
Correspondence: daniel.chuquin@espoch.edu.ec

Article Info

Page Number: 730 - 748

Publication Issue:

Vol 72 No. 1 (2023)

Abstract

The present study aims to design an Artificial Neural Network (ANN) to estimate the mole fractions resulting from the non-catalytic esterification process of Free Fatty Acids (FFA) that compose Karanja oil. The ANN was designed in the MATLAB program based on 100 pairs of data samples generated by a simulation validated in the free software DWSIM. Through a sensitivity analysis, it was determined that the inputs of the ANN were: the water mole fraction of stream 1C (1C-Xa), the oleic acid mole fraction of stream 3C (3C-Xo), the percentage conversion of the chemical reaction (%C), and the pressure drop in the reactor (-p). The methyl oleate mole fraction (9C-XM-O), methanol mole fraction (9C-Xm), triolein mole fraction (9C-XOOO), and trilinolein mole fraction (9C-XLLLL) from the liquid stream are established as outputs of the ANN. The mole fraction of methanol (10C- Xm) and the mole fraction of water (10C- Xa) from the gaseous stream. The ANN was trained and validated with a Bayesian regularization algorithm (30 hidden neurons) from which a mean squared error (MSE) = 0.00000411 and a total regression coefficient (R) of 0.99 were found. With these results and through the application of an ANOVA-type statistical analysis, it was determined with 95% reliability that the ANN has a good predictive capacity, which can be applied in the prediction of free fatty acids in the production of second-generation biodiesel (FAME).

Article History

Article Received: *15 October 2022*

Revised: *24 November 2022*

Accepted: *18 December 2022*

Keywords: Chemical Engineering Sciences and Technology; Free Fatty Acids (FFA); Oleic Acid (O); Methyl Oleate (MO); DWSIM; MATLAB; Artificial Neuronal Networks (ANN)

1. 1. Introduction

For decades, oil and non-renewable energies have been the basis of the world's energy structure; due to their high level of consumption, they have become the main driving force in both developed and developing countries. For example, according to statistics, in the European Union (EU), 30% of unprocessed energy, i.e., primary energy, is used for transportation and 98% of this depends on fossil hydrocarbons (1).

Luque and Melero (1) mention that EU countries have established regulations that encourage the use of biofuels, and the results were significant since greenhouse gases decreased by 80% when using non-edible oil residues, i.e., second-generation materials, in contrast to pollutant emissions that are less than 50%, if only first generation raw materials are used. In this aspect, fatty acid metal esters (FAME) become an alternative source of energy (green fuels) which are obtained from renewable sources, such as the oily composition of vegetable and animal oils and fats (2). Romero (3) argues that FAME is characterized by being renewable, biodegradable, and having lower toxicity than table salt; its high lubricity and its intrinsically sulfur-free content, compared to diesel, favors the energy efficiency of combustion and doubles the life of engines, without requiring any modification in them (4). Low-sulfur diesel is usually mixed with a certain amount of FAME to improve its lubricating power. In countries such as Colombia, for example, the government created Law 939 in 2004, which establishes that diesel fuel must initially be of type B05, i.e., the FAME content in diesel fuel must be 5% (5). India has also implemented a program for large-scale production of FAME with a 20% gasoline blend (6).

1.1. FAME Production Processes

This study will focus on producing a second-generation long-chain ester compound (C14-C24), which means that it can be obtained from non-edible oils or from commercial or domestic oil residues that are processed to take maximum advantage of its composition (7). In this case, the starting point will be inedible oil.

Singh et al. (8) state that there are several methods to obtain FAME, among them thermal cracking, based on any raw material of different generations. FAME has high ash and carbon residues, exceeding the acceptable margin. In addition, the thermal requirement makes the process inefficient. The current technology for obtaining FAME is the transesterification of non-edible vegetable oils, together with alkalis, including potassium hydroxides, sodium hydroxides and compounds known as alcoholates (1,9).

Using homogeneous alkaline catalysts involves certain drawbacks in producing FAME because it cannot be reused. Ultimately, it separates into 2 phases (glycerol and soap). Therefore, it hinders the purification of glycerol and decreases the yield of FAME production (10).

Lee et al. (11) determined that the production of FAME on an industrial scale is preferably carried out from heterogeneous alkaline catalysts, especially when the oil is of high purity and contains low portions of free fatty acids (FFA), due to their faster reaction speeds, about the acid catalysts. Moreover, heterogeneous alkaline catalysts are ideal for synthforizing FAME concerning homogeneous alkaline catalysts (8).

1.2. Karanja Oil

Orange oil is rich in free fatty acids (FFA), which are exploited through transesterification processes by catalytic routes to produce alkyl esters (12,13). However, esterification with the influence of homogeneous acid catalysts represents several disadvantages, such as corrosion of the equipment, difficulties in the purification of the product and the recovery of the catalysts. To this is added the high requirement of temperature and pressure in its operation (14).

Due to the problems presented by the use of acid catalysts, Minami and Saka (15) analyzed non-catalytic supercritical conditions in the transesterification processes using supercritical methanol (critical T = 239 C, critical P = 8.09 MPa), where it was evidenced that transesterification occurs from the triglycerides of the oil and the FFA are simultaneously esterified. However, the operating parameters exceeded the critical conditions (350 C and 20 - 50 MPa), which generates an increase in operating costs and also, the product tends to degrade thermally. Therefore, according to Hussain et

al., esterification problems are minimized under subcritical conditions by employing non-catalytic esterification techniques (13).

1.3. ANNs applied in FAME procurement

For the prediction of certain complex non-linear processes that cannot be described with other methodologies because their results tend to be unstable, ANNs have become a tool for prediction due to their high accuracy and learning capacity (16).

Santana et al. (17) point out that ANNs are superior to other types of modeling because they do not require assumptions about the nature of a phenomenon, as with simulators. In addition, ANNs recognize the mathematical procedure and achieve the learning of linear and non-linear interactions between the dependent and independent variables of the proposed process from an initial experience and also organize the information captured at the beginning of the training.

Bourquin et al. (18) recognized the advantage of using an ANN in contrast to the response surface methodology (RSM) for analyzing the ejection force measurements exerted by the tablets. All determined ejection properties were mainly influenced by the concentration of magnesium stearate and silica aerogel, while the other factors showed much lower effects; these important relationships can only be recognized from the ANN model, while the RSM model ignored them.

ANNs are fault-tolerant since they can continue to process information, retaining certain parts of the network, even if destroyed, thanks to the redundancy of data formation. They are dynamic, and their insertion is straightforward with current technology (17). They provide a better quality of adjustment to the experiment due to the great flexibility caused by the various mathematical functions that this non-linear modeling has (19).

ANNs have been used in producing FAME to such an extent that it is possible to verify its quality by analyzing its chemical composition. Kinematic viscosity, for example, is a predicted property that reveals the state of atomization that the fuel (FAME) will have, the fuel-air ratio and the combustion efficiency. The main indicator of this property is the length of the carbon chain of FAME; as the carbon chain increases, the kinematic viscosity will increase in direct proportion (20).

Suresh et al. developed an ANN for producing FAME using the ultrasonication time, the added CuO loading and the methanol-oil molar ratio as input variables. The dependent variable was the FAME yield. The optimized parameters obtained by ANN to obtain the highest FAME yield (97.82%) were 35 to 36 minutes in the ultrasonication stage, the catalyst loading was 2.07 wt%, and the methanol-oil molar ratio resulted in 29.87:1 (21).

Garg & Jain (22) collected the necessary information for optimizing the process parameters of FAME production from the lipid composition of algae. The production was modeled using the Levenberg-Marquardt (LM) algorithm for ANN training and learning. In contrast, with the response surface method (RSM), the ANN presented a better performance in predicting the results. The performance parameter evaluated was the coefficient of determination (R2), which for ANN was 0.999, while for RSM, it was 0.965.

Oladipo et al. (23) developed an ANN for producing FAME from neem oil, jatropha and used cooking oils. The software used was MATLAB R2017a, and the ANN was trained with the LM algorithm. The statistical performance values of the ANN were: RMSE = 0.00256 and R2 = 0.996, so it was established that the ANN presents a high degree of reliability in its predictions.

Teo SH et al. (24) evaluated and optimized the production of FAME using ANN and genetic algorithms. They used crude oil from Jatropha curcas, a high FFA oil, which, when combined with a

synthesized catalyst derived from eggshell waste, resulted in the formulation of FAME with a maximum yield (98%) through glycerolysis and transesterification reactions with methanol at atmospheric pressure.

On the other hand, Hafiidz et al. (25) employed an ANN to optimize the production of FAME from the esterification of FFA from oleic acid, catalyzed by the ionic liquid 1-butyl-3-methylimidazolium hydrogen sulfate ([BMIM] [HSO4]) compound. As a result, FAME and O2 conversion yield using this technique was 81.2% and 80.6%, respectively.

The objective of this study is to develop an ANN with the ability to predict the mole fractions of FAME from inedible oils (Karanja oil). The ANN will be developed from the simulation of the FAME production process proposed by (13), taking into account the operating conditions of the process. Future studies will be developed to incorporate the ANN into an industrial plant to optimize and continuously improve the processes.

2. Materials and Methods

Process Description

The simulation of the process corresponding to the non-catalytic esterification of FFA was carried out using the DWSIM software, taking as a reference the study developed by (13). Figure 1 describes the process used for the production of FAME.

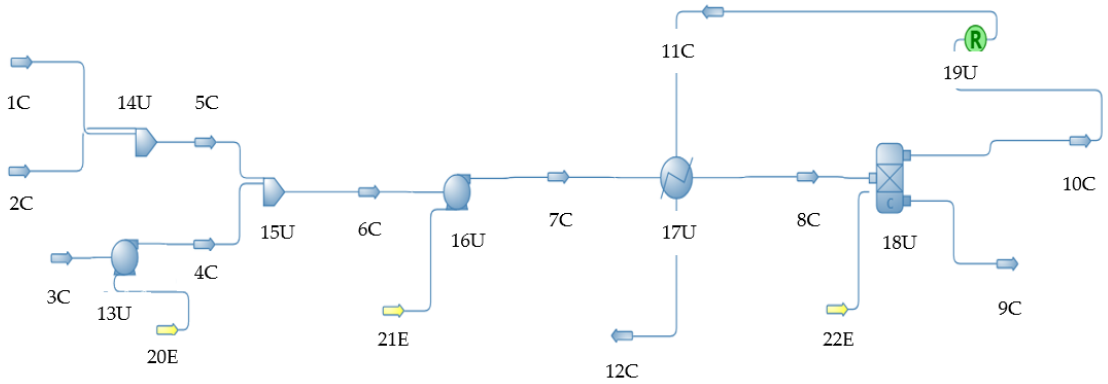

Figure 1. Diagram of the non-catalytic esterification process of FFA simulated in the DWSIM program.

Nomenclature: 1C: Feed 1; 2C: Feed 2; 3C: Oil; 4C: Stream 1; 5C: Stream 2; 6C: Stream 3; 7C: Reagents 1; 8C: Reagents 2; 9C: Methyl Oleate; 10C: Methanol+Water 1; 11C: Methanol+Water 2; 12C: Methanol+Water 3; 13U: Pump 1; 14U: Mixer 1; 15U: Mixer 2; 16U: Pump 2; 17U: IC (heat exchanger); 18U: Reactor; 19U: Block R; 20E: Energy B1; 21E: Energy B2; 22E: Energy R.

Stream 3C (1050 kg/h), consisting of oxygen (60.7%) and triglycerides (TG), is pumped to a mixer (15U), which additionally receives a stream (5C), resulting from the mixing of two streams, the first containing methane mole fractions (1C) and the second consisting only of methane (2C). This mixture (7C) passes through a countercurrent heat exchanger (17U) operating at 26 kW in order to take advantage of the heat generated in the reaction (10C). After the heat exchanger, the mixture enters the conversion reactor (18U), where 99.85% O2 conversion occurs. Table 1 details the operating parameters and compositions of the streams used in the simulation process.

Table 1. Parameters of process operation

Parameters	**1C**	**2C**	**3C**	**11C**	**17U**	**18U**
Pressure (bar)	1	1	1		-	-
Temperature (°C)	64,54			220	-	-
Molar flow (Kmol/s)	155,33	2,81	2,02	158,03	-	-
Mass flow (Kmol/s)	4976,96	90,11	1050	5146,63	-	-
Molar composition					-	-
OOO	-	-	0,217	3,53E-04	-	-
O	-	-	0,607	0	-	-
m	0,99	1	-	0,99	-	-
a	1,13E-4	-	-	7,85E-03	-	-
M-O	-	-	-	1,26E-03	-	-
AAA	-	-	0,020	-	-	-
SSS	-	-	0,017	-	-	-
LLL	-	-	0,108	-	-	-
PPP	-	-	0,028	-	-	-
Heat exchange area (m^2)	-	-	-	-	1	-
Heat exchanged (kW)	-	-	-	-	26	-
Outlet temperature (°C)	-	-	-	-	-	220
Pressure drop (bar)	-	-	-	-	-	-13
Job (kW)	-	-	-	-	-	2090,24
Oleic Acid Conversion	-	-	-	-	-	99,85

OOO: triolein, O: oleic acid, m: methanol, a: water, M-O: methyl oleate, PPP: tripalmitin, SSS: tristearin, LLL: trilinolein, AAA: triaraquidine. - shows values that have been obtained thanks to the execution of the program or simply do not correspond to that section.

Source: (13)

148 *2.2. Methodology*

149 Figure 2 summarizes the methodological procedure used for the design of the ANN. The first step is
150 to simulate the non-catalytic esterification process of FFA in DWSIM based on the operating
151 parameters of Table 1, the simulation is validated, and a sensitivity analysis is performed to
152 establish the dependent and independent variables of the process. Then, the database used for the
153 ANN's design, training and validation is constructed. Finally, a statistical analysis is performed to
154 determine the reliability of the prediction system of the resulting mole fractions of the FAME
155 production process.

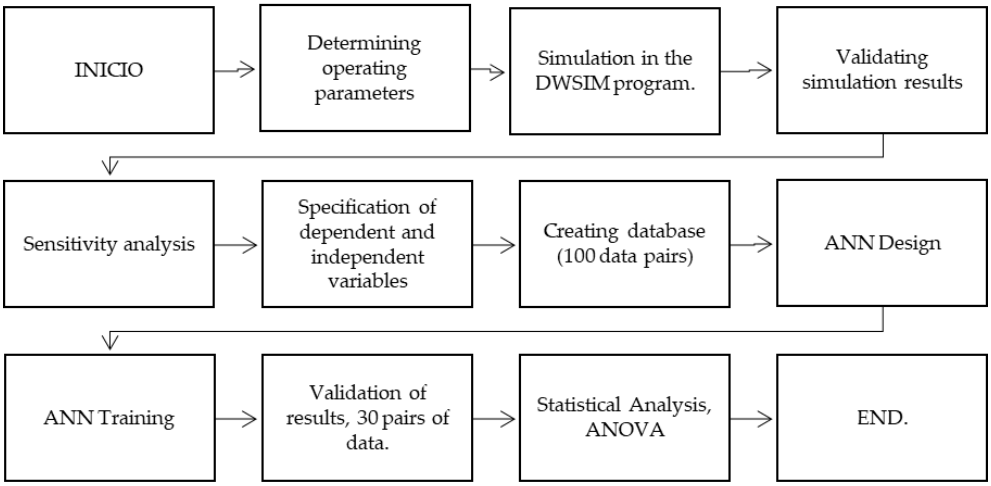

156

157 **Figure 2.** Methodological scheme for the design and validation of the NNA

158 *2.3. Simulation in DWSIM*

159 Santos & Van Gerven (26) consider that simulators such as Aspen Plus, Aspen Hysysys, UniSim,
160 CHEMCAD, and DWSIM, among others, are capable of modeling a plant at an industrial level and
161 that through them, a series of physical and chemical changes can be proposed without the need to
162 invest large amounts of money in training, configuration or optimization projects. Furthermore,
163 Madeiros (27) states that DWSIM (CAPE-OPEN compatible) has an easy-to-use graphical interface
164 and can simulate processes in steady or dynamic states. In addition, it allows for performing
165 sensitivity analyses, which provide a deep understanding of the process behavior up to the point of
166 reaching its optimal state.

167 For the simulation in DWSIM of the non-catalytic esterification process of free fatty acids that
168 compose the Karanja oil, the operating parameters established in Table 1 were taken into account,
169 using Raoult's Law as a thermodynamic package, which was adequately adjusted to the non-catalytic
170 esterification process of FFA. Raoult's Law is widely used in solutions that assume ideal behavior
171 and contain liquid and vapor phases (28).

172 *Sensitivity Analysis*

173 The following were analyzed as independent variables: the mole fraction of water in stream 1C (1C-
174 Xa), the mole fraction of oleic acid in stream 3C (3C- Xo), the pressure drop in the reactor (-p) and the
175 conversion percentage (%C) within the configuration of the chemical reaction, because they are those
176 variables that exert a significant influence on the responses of the dependent variables which are: the

mole fractions of methyl oleate (9C-XM-O), methanol (9C-Xm), triolein (9C-Xooo) and trilinolein (9C-XLLL), this for the 9C stream. The most important mole fractions within the 10C matter line are those of methanol (10C- Xm) and water (10C- Xa).

Table 2 establishes the operating limits of the independent variables used as inputs to the ANN:

Table 2. Operating limits for ANN inputs.

Operating Limits				
Parameter	Mole fraction a	Mole fraction O	Pressure drop (bar)	Conversion Rate (%)
Description	Current 1C	Current 3C	In the reactor	Chemical reaction properties
**Range*	0 a 1	0 a 1	-1 a -35	0 a 100

2.3. Design and training of the ANN

Figure 3 details the design of the ANN, which was created using the MATLAB Neural Network Toolbox, version R2017b. The structure of the ANN consists of an input layer of 4 neurons corresponding to the independent variables established in the sensitivity analysis: (1C- Xa), (3C- Xo), (-p), (%C). The ANN has a hidden layer with 30 neurons and 6 neurons in the output layer, which are the dependent variables of the non-catalytic esterification process: (9C-XM-O), (9C-Xm), (9C-Xooo), (9C-XLLL), (10C- Xm), (10C- Xa).

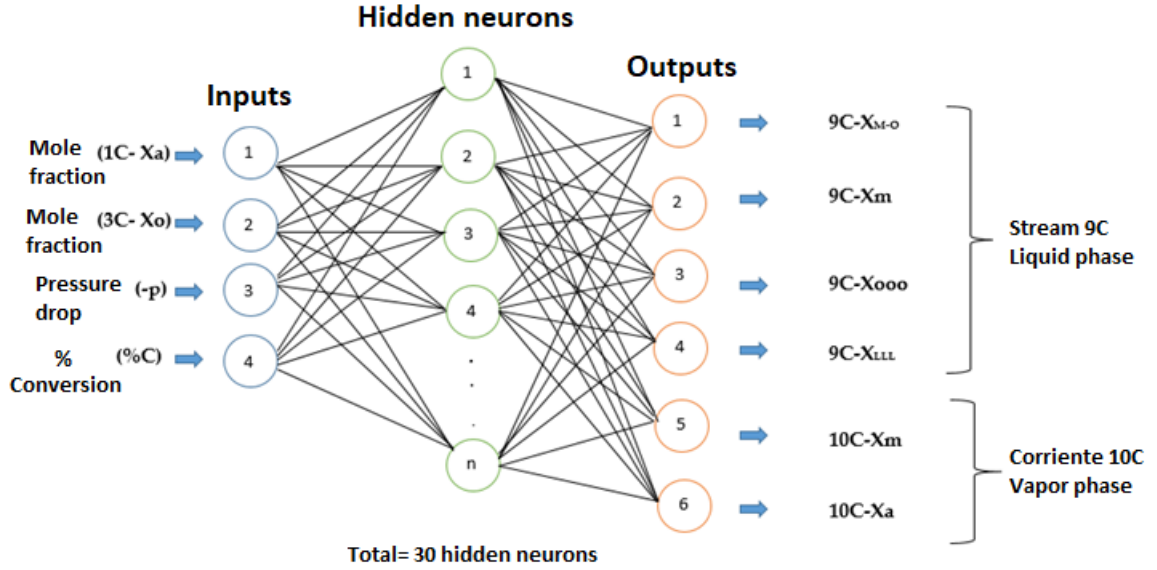

Figure 3. Schematic of the designed ANN

Based on the guide proposed by Chen et al. (29), for learning, training and validation of the network, 70% of the total data pairs were used, while 30% were used to perform a test to evaluate its learning level. ANN training adjusts the weights of the connections between neurons so that the ANN makes appropriate predictions for the target output data. Validation measures the ANN's prediction errors to

evaluate its performance. Finally, testing evaluates ANN prediction using pairs of data not used in the training process (30).

3. Results and Discussion

3.1. Validation of the simulation

To validate the simulation performed in DWSIM, the results were compared with the work developed by Hussain & Kumar (13) in AspenPlus; the outputs of the most relevant mole fractions of the 9C and 10C stream and the temperature of the 12C stream were taken into account. Table 3 shows the comparison of the results obtained. The calculated percentage errors (%E) are below 6%, indicating the reliability of the simulated process.

Table 3. Simulation validation

Conversion Reactor				
Currents	**Mole fractions**	**ASPEN PLUS -13**	**DWSIM**	**E (%)**
10C	Xm	0.99	0.99	0%
	Xa	7.85E-03	7.88E-03	0.38%
9C	X_{M-O}	0.481	0.504	4.78%
	Xm	0.17	0.16	5.88%
	X_{OOO}	0.179	0.184	2.79%
	X_{LLL}	0.103	0.097	5.82%
Heat Exchanger				
Currents	**Temperature (°C)**	**ASPEN PLUS -13**	**DWSIM**	**E (%)**
12C	Hot Fluid	210.5	209.9	0,28%

3.2. Sensitivity Analysis

The sensitivity analysis enabled it to detect four independent variables that representatively affect the six dependent variables. To determine the influence of the independent variables, the analysis was performed on the dependent variable of greatest interest (9C-XM-O). For example, Figure 4 shows the change of the variable 9C-X_{M-O} for the 1C-Xa stream (composed of water and methanol); the change is inversely proportional as the amount of water in the 1C-Xa stream increases, the methanol fraction decreases, and this generates that the esterification reaction is limited by the amount of methanol present in the medium. On the other hand, Figure 5 shows that the dependent variable 9C-XM-O is directly proportional to independent 3C-Xo, because the production of FAME depends on the amount of methyl oleate.

Pressure drop is also a sensitive variable to the process; as seen in Figure 6, there is an inversely proportional correlation between the independent variable -p, and the dependent variable 9C-XM-O.

Using this analysis, it was possible to know the behavior of the process and to delimit the optimum pressure ranges within the conversion reactor so as not to impair the esterification. Finally, in Figure 7 it can be seen that the conversion percentage strongly influences the esterification process, presenting a directly proportional relationship. As the conversion percentage increases in the reactor, the production of FAME increases.

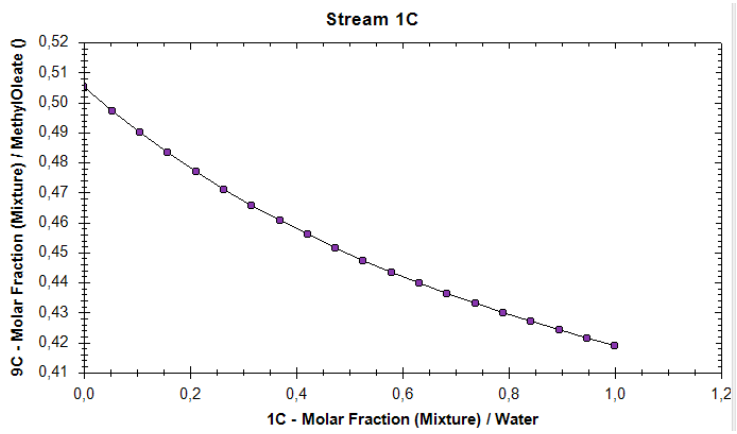

Figure 4. Impact of the variable 1C-Xa on the variable 9C-$X._{M-O}$

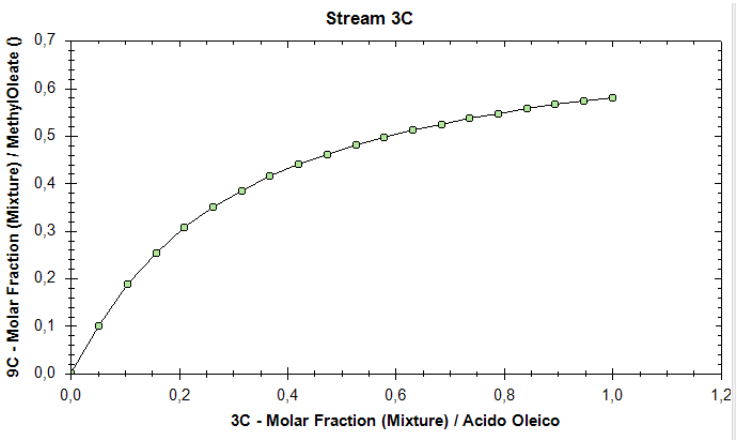

Figure 5. Incidence of the variable 3C- Xo on the variable 9C-$X_{M-O.}$

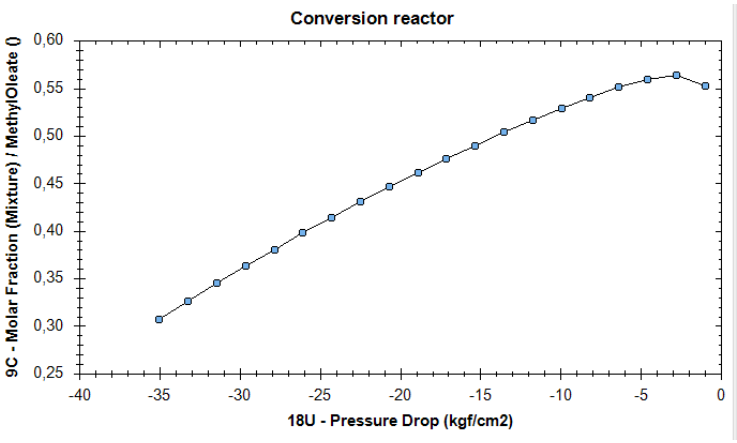

Figure 6. Incidence of the variable -p versus the variable 9C-$X._{M-O}$

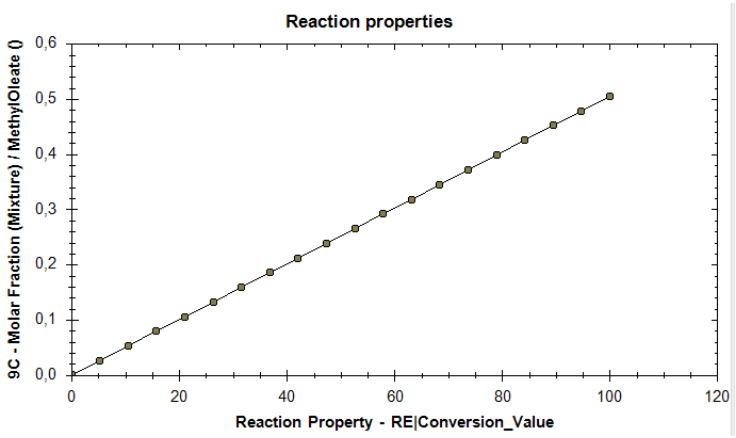

Figure 7. Incidence of the variable %C on the variable 9C-$X_{M\text{-}O}$.

3.3. ANN topology

The hidden neurons of the intermediate layer were determined through an experimental trial by varying the number of neurons and the training algorithm, evaluating the ANN performance with quantitative performance indicators (MSE and R). Table 4 summarizes the tests performed for the performance parameters. Bayesian networks (BR) discard the validation phase due to the robustness of this type of backpropagation network, which can discard the data designated for validation and take advantage of them in the relevant stages, such as training and learning. However, using the BR algorithm with 60 neurons, abnormal behavior is detected in training MSE since the error is deficient, indicating that the ANN is probably not learning but memorizing the data. In this sense, it is essential to find a balance (MSE and R values) between training and testing so that the ANN has a good prediction capacity.

Table 4. R and MSE values in the experimental trials.

Testing	Algorithm	# of neurons	Indicators	Train	Validation	Test
1	*LM**	60	*MSE*	2,01-06	5,43E-03	1,10E-02
			R	0,99	9,59E-01	9,29E-01
2	*BR*	30	*MSE*	4,11*E-06	-	3,56*E-03
			R	9,99*E-01	-	9,76*E-01
3	*BR*	60	*MSE*	6,85E-13	-	1,76E-03
			R	9,99E-01	-	9,87E-01

LM: *Levenberg-Marquardt; BR*: Bayesian regularization.*

The training with the Bayesian Regularization (BR) algorithm is ideal for processing very noisy or complicated data; it works from the understanding of the parameters in the form of probabilities so that the weights of the network result from a set of probabilities that help to reduce prediction errors, offering an excellent generalized model (31) . Furthermore, Feng et al. (32) indicate that the BR algorithm is adaptive and can identify soft or sparse forces without any initial contextualization. In addition, the BR algorithm avoids the problem of overfitting and data memorization (33).

The ANN was designed with MATLAB NNTOOL, and it is composed of three (4) input neurons, a hidden layer with 30 neurons and six (6) output neurons. According to the study developed by Abiodum et al. (34), a hidden layer may be sufficient for prediction in most ANN applications.

3.3.1 ANN training and testing

The MSE values for the training and testing phase are 4.11E-06 and 3.56E-06, respectively, indicating that the ANN performs adequately and that the predictions are made with sufficient accuracy. Figure 8 shows the mean square error (MSE) evolution during the training phase, with a final MSE of 0.0036. The MSE performance function for the training data (train) is very close to zero, indicating that the predictive capability of the network is very good.

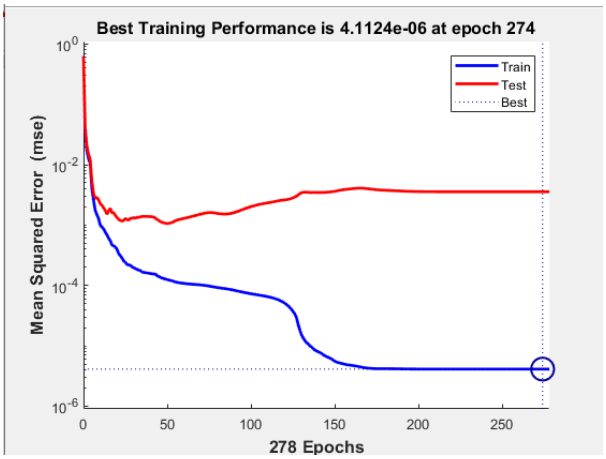

Figure 8. ANN training performance (MSE)

On the other hand, as seen in Fig.9, there is no dispersion between the outputs and targets of the ANN in both the training and test phases. The R values for the training and testing phase are 0.999 and 0.976, respectively, which indicates that the outputs and targets have an acceptable correlation. Therefore, for validating the ANN, the decision was made that the R-value should be in the range of 0.95 to 1 and the MSE lower than 0.025.

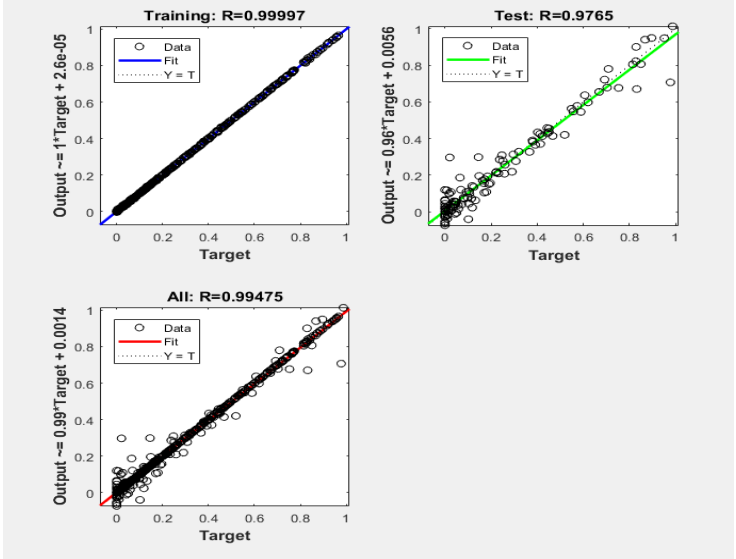

Figure 9. Regression coefficient R for ANN training and testing

3.4. ANN model prediction

Figures 10 - 11, 12 - 13 and 14 - 15 correspond to the resulting mole fraction plots of both the liquid stream (XM-O, Xm, XOOO, XLLL) and the gaseous stream (Xm, Xa), comparing the data collected from the DWSIM simulations or actual values (blue line) and the data predicted by ANN (red line). Based on the observations in the figures, it can be interpreted that there is no significant difference between the predicted and actual data for each of the output variables. Furthermore, the lag or presence of outliers between the two curves is minimal.

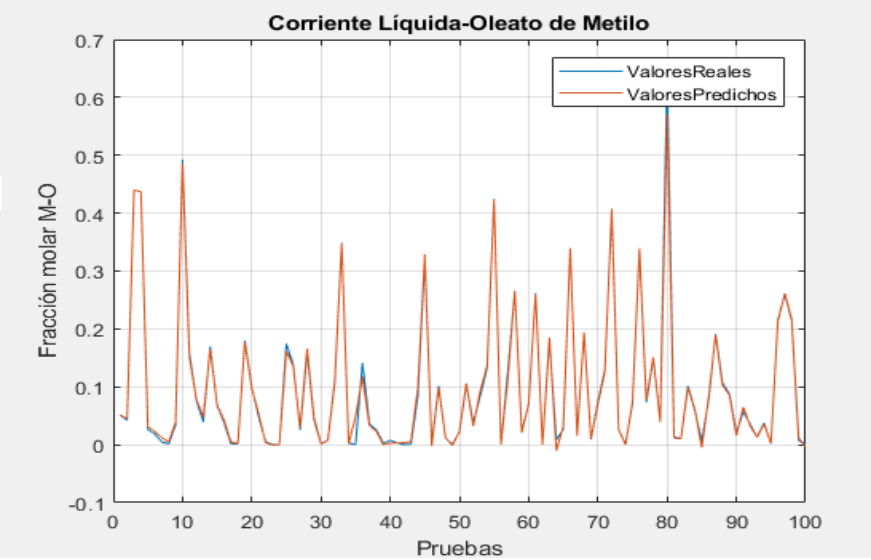

Figure 10. M-O mole fraction of the liquid stream, actual (DWSIM) vs. predicted (ANN)

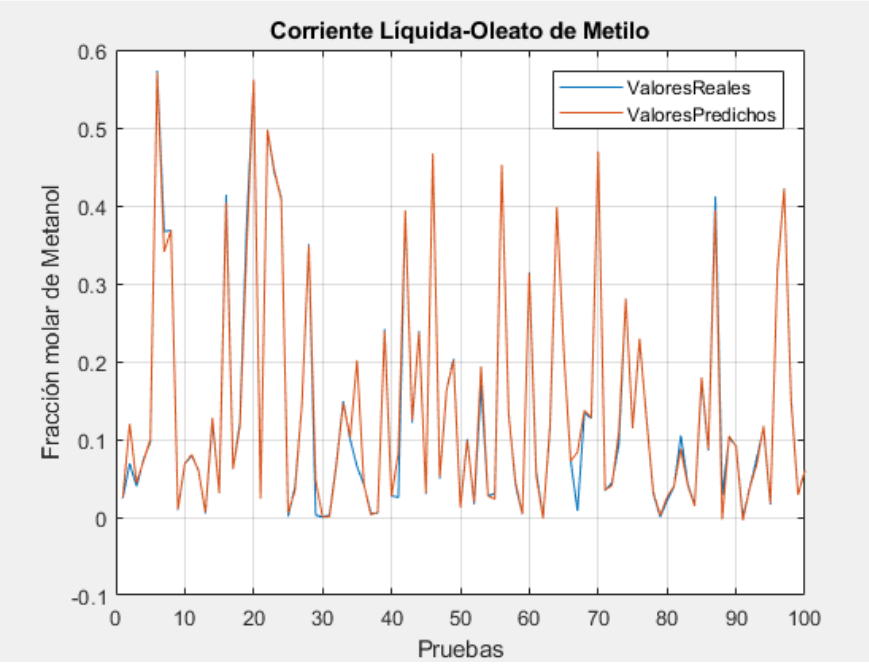

Figure 11. Mole fraction of m of the liquid stream, actual (DWSIM) vs. predicted (ANN)

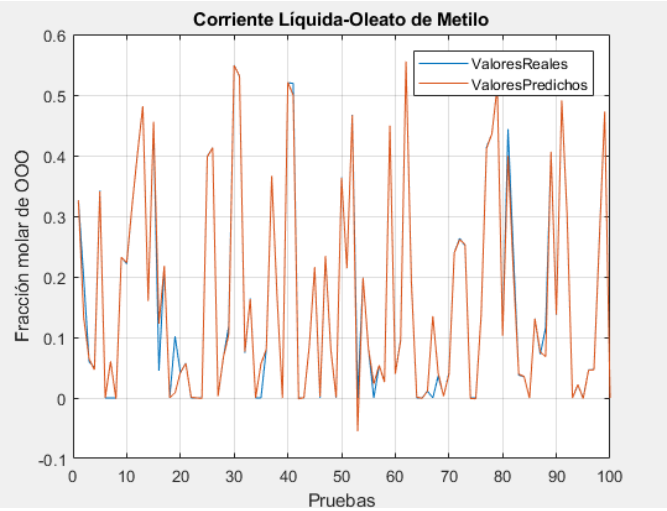

Figure 12. OOO mole fraction of the liquid stream, actual (DWSIM) vs. predicted (ANN)

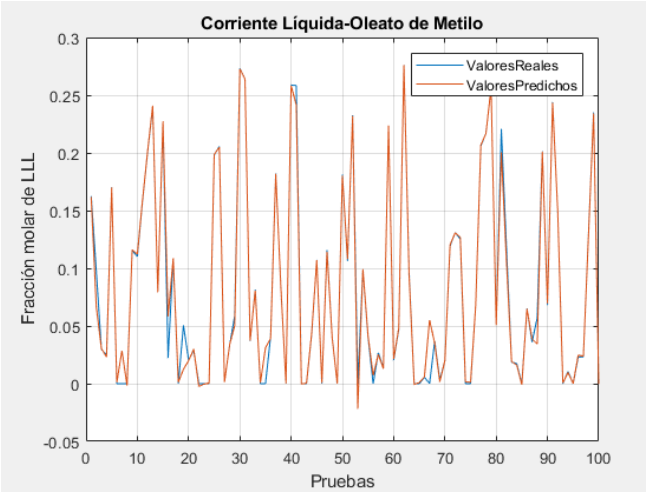

Figure 13. LLL mole fraction of the liquid stream, actual (DWSIM) vs. predicted (ANN)

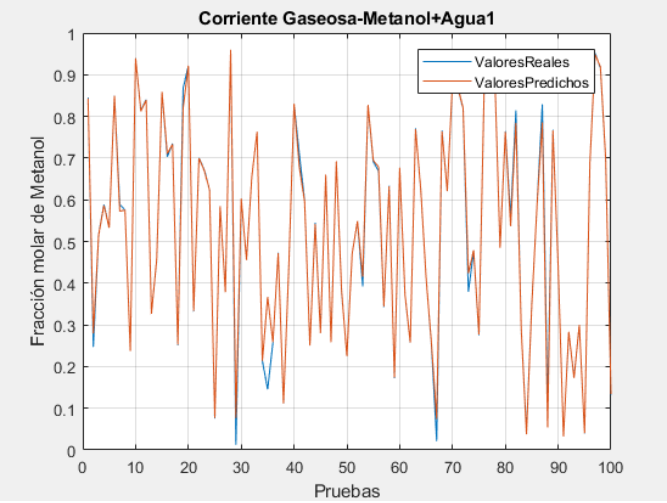

Figure 14. Mole fraction of m of the gaseous stream, actual (DWSIM) vs predicted (ANN)

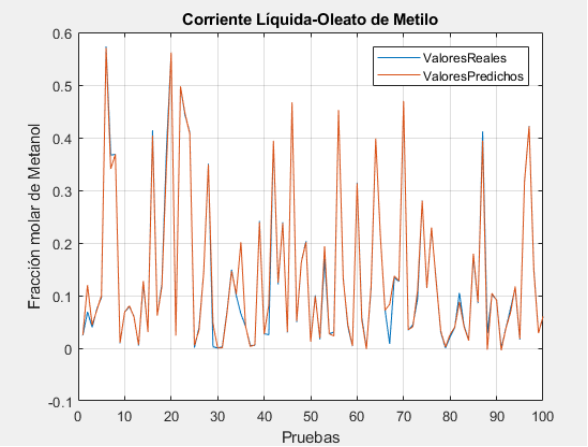

Figure 15. Water mole fraction of the gaseous stream, actual (DWSIM) vs. predicted (ANN)

3.5. ANN model verification

The ANN predictive was tested with a set of 30 random input data unknown by the ANN. The results show an overlap between the experimental data and the predictions. This indicates that ANN has an excellent predictive capacity for the dependent variables. The Figure shows the prediction of the variables under study by the ANN for the experimental data that were not considered in the network learning process.

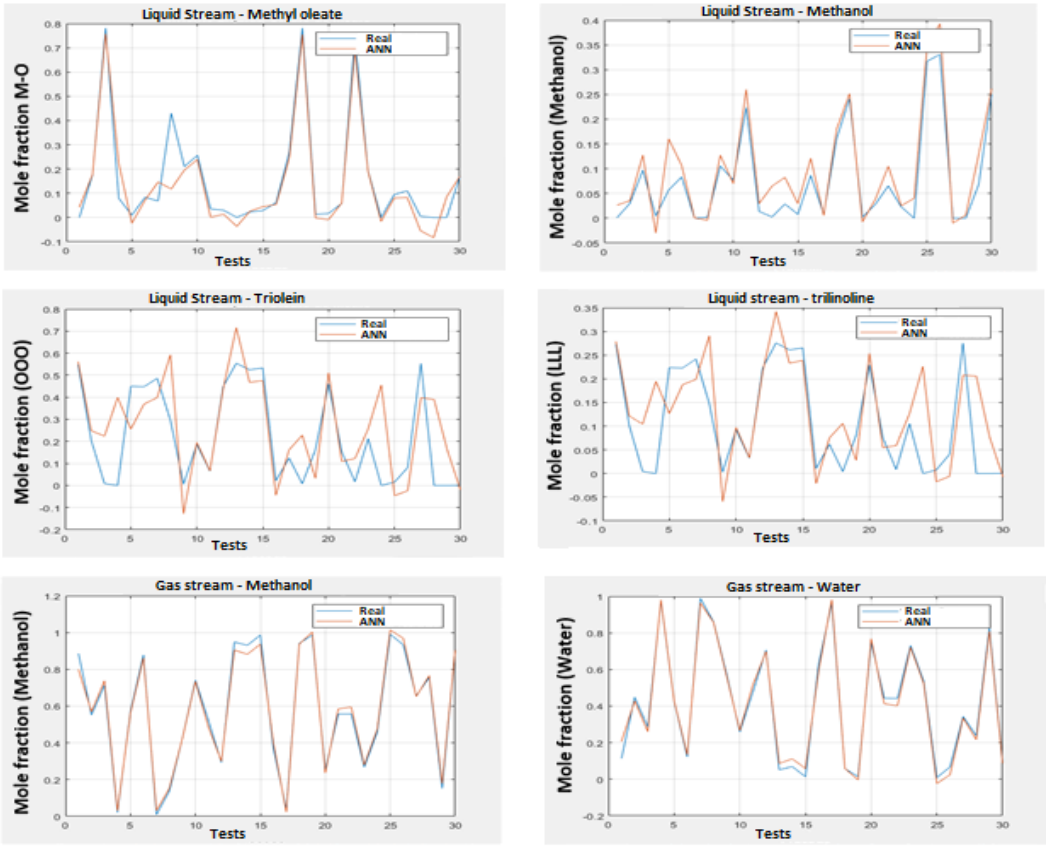

Figure 16. Comparison between actual and predicted outputs of each stream. Liquid stream-9C: a) Mole fraction M-O, b) Mole fraction m, c) Mole fraction OOO, d) Mole fraction LLL. Gaseous stream-10C: a) Mole fraction m, b) Mole fraction a.

The research used the function ANOVA to validate the ANN statistically. Table 5 shows the results from ANOVA. For all cases, P-values (probability value in statistical significance tests) is greater than 0.05, indicating no statistically significant difference between the means of the observations and the predictions. These statistical tests reveal that the ANN constructed is statistically valid for predicting the mole fractions of methyl olein, methanol, triolein, water and trilinoline, with a confidence level of 95%.

Table 5. ANOVA

Source	Sum of squares	DOF	Mean square	F- value	P- value
M-O mole fraction of the 9C stream					
Inter groups	0,00386988	1	0,00386988	0,08	0,7837
Intra groups	2,9522	58	0,0509		
Total (Corr.)	2,95607	59			
Mole fraction of m of the current 9C					
Inter groups	0,00721209	1	0,00721209	0,66	0,4196
Intra groups	0,632883	58	0,0109118		
Total (Corr.)	0,640095	59			
Mole fraction of OOO of the 9C current					
Inter groups	0,0328439	1	0,0328439	0,69	0,4082
Intra groups	2,74497	58	0,0473271		
Total (Corr.)	2,77782	59			
LLL mole fraction of the current 9C					
Inter groups	0,00828621	1	0,00828621	0,72	0,3999
Intra groups	0,668125	58	0,0115194		
Total (Corr.)	0,676411	59			
Mole fraction of m of the current 10C					
Inter groups	2,61662E-7	1	2,61662E-7	0,00	0,9987
Intra groups	5,97879	58	0,103083		

Total (Corr.)	5,97879	59			
Mole fraction of a of current 10C					
Inter groups	0,0000417794	1	0,0000417794	0,00	0,9841
Intra groups	6,01191	58	0,103654		
Total (Corr.)	6,01196	59			

4. Conclusions

In this paper, an ANN capable of predicting the mole fractions derived from a non-catalytic esterification process of FFA to obtain FAME was structured, taking as a starting point a set of 130 pairs of data processed in DWSIM. The ANN input variables were; the mole fraction of an of stream 1C (1C- Xa), the mole fraction of O of stream 3C (3C- Xo), the percentage conversion of the chemical reaction (%C) and the pressure drop in the reactor (-p), which resulted in the prediction of 6 output variables; the mole fraction of M-O (9C-XM-O), the mole fraction of m (9C-Xm), the mole fraction of OOO (9C-XOOO) and the mole fraction of LLL (9C-XLLLL) of the liquid stream 9C, the mole fraction of m (10C-Xm) and the mole fraction of a (10C- Xa) of the gaseous stream 10C.

The network was trained with the Bayesian regularization algorithm, and its design consists of 30 neurons with a running performance of MSE = 4.11*E-06 and R = 0.99. A statistical comparison analysis (ANOVA) between the experimental data (DWSIM) and the values predicted by the neural network was also used to validate the ANN. Statistical tests (P-value > 0.05) show that the ANN accurately predicts the mole fractions at the outputs with a 95% significance level. According to the results, this tool can be handy for large-scale FAME production, taking advantage of the FFA composition in commercial or domestic waste oils. For instance, real operating parameters of the described process must be used as input, apply them in situ and verified the predictions at the control points (outputs of the ANN).

Supplementary Materials: The following are available online at www.mdpi.com/xxx/s1, Figure S1: title, Table S1: title, and Video S1: title.

Author Contributions: Conceptualization, D.CH.V and A.S; methodology, W.D, and D.CH.V ; software, W.D, N.CH.V and J.CH.V; ANN, N.CH.V and J.CH.V; validation, D.CH.V and A.S; formal analysis, D.CH.V and C.C.T; statistical analysis, N.CH.V and J.CH.V, data curation, D.CH.V and A.S.; writing-original draft preparation, D.CH.V and A.S; writing-review and editing, D.CH.V and C.C.T; supervision, C.C.T; funding acquisition, N.CH.V, J.CH.V, D.CH.V. All authors have read and agreed to the published version of the manuscript.

Acknowledgments: The author thanks the Security Research Group on Environment and Engineering, “GISAI” for allowing the execution of this research.

Conflicts of Interest: The authors declare no conflict of interest.

References

1. Luque R, Melero JA. Introduction to advanced biodiesel production. In: Advances in Biodiesel Production. Elsevier; 2012. p. 1–9.

2. Vargas EM, Ospina L, Neves MC, Tarelho LAC, Nunes MI. Optimization of FAME production from blends of waste cooking oil and refined palm oil using biomass fly ash as a catalyst. Renew Energy. 2021;163:1637–47.

3. Loaiza Romero FE. Cinética de la reacción de transesterificacién del aceite de higuerilla en la obtención de biodiesel. 2003. p. 129.

4. Kumar S, Razali M, Farabi MSA, Izham M, Zainal Z, Taufiq-yap YH. Production of methyl esters from waste cooking oil and chicken fat oil via simultaneous esterification and transesterification using acid catalyst. Energy Convers Manag. 2020;226(October):113366.

5. González AF, Jiménez IC, Rodríguez Susa M, Restrepo S, Gómez JM. Biocombustibles de segunda generación y Biodiesel: Una mirada a la contribución de la Universidad de los Andes. Rev Ing. 2008 Nov;0(28):70.

6. Axelsson L, Franzén M, Ostwald M, Berndes G, Lakshmi G, Ravindranath NH. Perspective: Jatropha cultivation in southern India: Assessing farmers' experiences. Biofuels, Bioprod Biorefining. 2012;6(3):246–56.

7. Mofijur M, Siddiki SYA, Shuvho MBA, Djavanroodi F, Fattah IMR, Ong HC, et al. Effect of nanocatalysts on the transesterification reaction of first, second and third generation biodiesel sources- A mini-review. Chemosphere. 2020;128642.

8. Singh D, Sharma D, Soni SL, Inda CS, Sharma S, Sharma PK, et al. A comprehensive review of physicochemical properties, production process, performance and emissions characteristics of 2nd generation biodiesel feedstock: Jatropha curcas. Fuel. 2021;285(April 2020):119110.

9. Leung DYC, Wu X, Leung MKH. A review on biodiesel production using catalyzed transesterification. Appl Energy. 2010;87(4):1083–95.

10. Berrios M, Martín MA, Chica AF, Martín A. Study of esterification and transesterification in biodiesel production from used frying oils in a closed system. 2010;160:473–9.

11. Lee AF, Bennett JA, Manayil JC, Wilson K. Heterogeneous catalysis for sustainable biodiesel production via esterification and transesterification. Chem Soc Rev. 2014;43(22):7887–916.

12. Chai M, Tu Q, Lu M, Yang YJ. Esteri fi cation pretreatment of free fatty acid in biodiesel production , from laboratory to industry. Fuel Process Technol. 2014;125:106–13.

13. Hussain Z, Kumar R. Esterification of free fatty acids: experiments, kinetic modeling, simulation & optimization. Int J Green Energy. 2018;15(11):629–40.

14. Lou WY, Guo Q, Chen WJ, Zong MH, Wu H, Smith TJ. A highly active bagasse-derived solid acid catalyst with properties suitable for production of biodiesel. ChemSusChem. 2012;5(8):1533–41.

15. Minami E, Saka S. Kinetics of hydrolysis and methyl esterification for biodiesel production in two-step supercritical methanol process. 2006;85:2479–83.

16. Lamanna R, Gimón R. Neural predictive control by instantaneous linearization. RIAI - Rev Iberoam Autom e Inform Ind. 2007;4(2):90–7.

17. Santana JCC, De Araújo SA, Biazus JPM, De Souza RR. Simulación del proceso de biodegradación de aguas residuales de la industria de carne mediante una red neuronal artificial perceptrón multicapa Simulation of biodegradation process of wastewater from meat industry by means of a multilayer perceptron artif. Rev Chil Ing. 2015;23(2):269–75.

18. Bourquin J, Schmidli H, Hoogevest P Van, Leuenberger H. technique for data sets showing non-linear relationships using data from a. 1998;7:5–16.

19. Tesli N, Bojani N, Taka A, Zekovi Z. Chemical Engineering & Processing : Process Intensi fi cation Defatted wheat germ as source of polyphenols — Optimization of microwave- assisted extraction by RSM and ANN approach. 2019;143(June).

20. Jahirul MI, Rasul MG, Brown RJ, Senadeera W, Hosen MA, Haque R, et al. Jo ur l P re of. Renew Energy. 2020;

21. Suresh T, Sivarajasekar N, Balasubramani K. Jo ur na l P re of. Renew Energy. 2020;

22. Garg A, Jain S. Process parameter optimization of biodiesel production from algal oil by response surface methodology and artificial neural networks. Fuel. 2020;277(February):118254.

23. Oladipo AS, Ajayi OA, Oladipo AA, Azarmi SL, Nurudeen Y, Atta AY, et al. Magnetic recyclable eggshell-based mesoporous catalyst for biodiesel production from crude neem oil: Process optimization by central composite design and artificial neural network. Comptes Rendus Chim. 2018;21(7):684–95.

24. Teo SH, Islam A, Reza H, Masoumi F, Taufiq-yap YH. SC. Renewable Energy. Elsevier Ltd; 2017.

25. Hafiidz A, Fauzi M, Aishah N, Amin S. Optimization of oleic acid esterification catalyzed by ionic liquid for green biodiesel synthesis. Energy Convers Manag. 2013;76:818–27.

26. Santos P, Van Gerven T. Aspen Hysys – Unity Interconnection. An Approach for Rigorous Computer- Based Chemical Engineering Training. In: Computer Aided Chemical Engineering. Elsevier B.V.; 2020. p. 2053–8.

27. Medeiros D. DWSIM - El simulador de procesos químicos de código abierto - Solo otro sitio de WordPress. 2021.

28. Manassaldi JI, Mussati MC, Scenna NJ, Mussati SF. Development of extrinsic functions for optimal synthesis and design — Application to distillation-based separation processes. Comput Chem Eng. 2019;125:532–44.

29. Chen Y, Song L, Liu Y, Yang L, Li D. A review of the artificial neural network models for water quality prediction. Appl Sci [Internet]. 2020;10(17). Available from: https://www.mdpi.com/2076-3417/10/17/5776

30. Chuquin-Vasco D, Parra F, Chuquin-Vasco N, Chuquin-Vasco J, Lo-Iacono- V. Prediction of methanol production in a carbon dioxide hydro- genation plant using neural networks . Energies [Internet]. 2021;14(13):1–18. Available from: https://www.mdpi.com/1996-1073/14/13/3965

31. Kayri M. Predictive abilities of Bayesian regularization and levenberg-marquardt algorithms in artificial neural networks: A comparative empirical study on social data. Math Comput Appl. 2016;21(2).

32. Feng W, Li Q, Lu Q, Li C, Wang B. Element-wise Bayesian regularization for fast and adaptive force reconstruction. J Sound Vib. 2021;490:115713.

33. Moshkbar-Bakhshayesh K. Performance study of bayesian regularization based multilayer feed-forward neural network for estimation of the uranium price in comparison with the different supervised learning algorithms. Prog Nucl Energy. 2020;127(May):103439.

34. Mustapha AN, Zhang Y, Zhang Z, Ding Y, Yuan Q, Li Y. Taguchi and ANOVA analysis for the optimization of the microencapsulation of a volatile phase change material. J Mater Res Technol. 2021 Mar;11:667–80.